


# The wear behaviour of different metallic bond alloys tested in a modified B611-13 test in an acidic, neutral and alkaline media

**Journal Article****Author(s):**

[Fabbro, Stefan](#) ; Kondratiuk, Jens; Tomandl, Alexander; Marra, Lucas; Kuffa, Michal; Wegener, Konrad

**Publication date:**

2023-04-15

**Permanent link:**

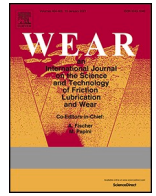
<https://doi.org/10.3929/ethz-b-000604970>

**Rights / license:**

[Creative Commons Attribution 4.0 International](#)

**Originally published in:**

Wear 518-519, <https://doi.org/10.1016/j.wear.2023.204651>



## The wear behaviour of different metallic bond alloys tested in a modified B611-13 test in an acidic, neutral and alkaline media

Stefan Fabbro<sup>a,\*</sup>, Jens Kondratiuk<sup>b</sup>, Alexander Tomandl<sup>b</sup>, Lucas Marra<sup>a</sup>, Michal Kuffa<sup>a</sup>, Konrad Wegener<sup>a</sup>

<sup>a</sup> Institute of Machine Tools and Manufacturing, ETH Zürich, Leonhardstrasse 21, 8092, Zürich, Switzerland

<sup>b</sup> Hilti AG, Feldkircherstrasse 100, 9494, Schaan, Liechtenstein

### ARTICLE INFO

#### Keywords:

Wear test  
B611-13 test  
pH  
Coefficient of friction  
Core drilling

### ABSTRACT

The abrasive and adhesive wear behaviour of metallic bonds can be significantly affected by varying pH values of the attacking medium. However, the knowledge about the pH value influence on diamond impregnated bits used in core drilling industry is still limited. One recent publication shows the advantage of modifying a standard ASTM B611-13 test to investigate the abrasive and adhesive wear behaviour of a diamond segment bond material in a neutral regime (pH7). This study mainly focuses on the effects of a varying surrounding media on the tribological behaviour using an acidic, neutral and alkaline slurry. This emulates more aggressive conditions for the diamond segments used in mining as well as construction industry. The pH value at which such diamond segments operate can differ from pH2 up to a value of pH13. The present work studies the wear behaviour of two metallic bonds in a modified B611-13 arrangement at 4 m/s sliding speed and different pH values. The tested specimens are investigated with regard to their change in mass and microstructure at the sliding interface zone. The results reveal a significant influence of the pH value on the wear behaviour of the bond system.

### 1. Introduction and state of the art

Diamond core drilling is an extensively used application in construction industry, mainly for drilling holes in reinforced concrete and rock material. As reported from Franca et al. [1], many different diamond cutting materials like polycrystalline diamond (PCD), surface set diamonds (SD) or impregnated diamond segments (ID) have been introduced in the past. They described diamond impregnated segments as the preferred option for drilling holes in hard and abrasive formations. Moseley et al. [2] highlight diamond core bits composed of diamond impregnated segments with typical diamond size of 300–600 µm embedded and randomly distributed in a metallic matrix with a diamond concentration between 5 and 20 vol%. Water at a flow rate of 1–4 l/min is used as a coolant for dissipating the heat and is necessary for flushing the concrete or rock slurry material out of the drilling hole. Miller et al. [3] reported in 1986 on the high importance of adjusting the bond matrix wear to the diamond wear to ensure the self-sharpening effect in order to keep the material removal efficiency stable. Tönshoff et al. [4] studied the wear behaviour of diamond segments during sawing experiments and described the contact characteristics between

the stone base material and the segment by distinguishing between bond wear and diamond wear. They observed erosive wear as a major wear characteristic on the segment wear. As rotational speeds in core drilling are approx. 30 times lower compared to circular sawing, the occurrence of erosive wear decreases significantly. Miller and Ball [5] as well as Xuefeng and Shifeng [6] investigated diamond wear in rock machining operations and found that abrasive wear and micro fracture of diamonds are present in impregnated diamond tools. The diamonds showed predominantly abrasive wear at low operational loads and mainly micro- or macro fracture at higher thrust force. In 2003, Borri-Brunetto et al. [7] characterized the abrasion properties of sintered tools with embedded hard particles describing the matrix material as main factor for retaining the embedded hard particles against pull-outs and therefore effect the cutting behaviour significantly. They concluded that the matrix wear is mainly influenced by the milling processes of the abrasive particles in the tool/base material interface. Due to the success of ID tools, considerable effort has been invested to understand the abrasive wear mechanisms of diamonds and the bond material, mainly focusing on stone cutting, sawing or drilling operations. The influence of different stone properties on bond wear of ID segments operated at different parameters

\* Corresponding author.

E-mail address: [fabbro@inspire.ethz.ch](mailto:fabbro@inspire.ethz.ch) (S. Fabbro).

<https://doi.org/10.1016/j.wear.2023.204651>

Received 8 August 2022; Received in revised form 29 January 2023; Accepted 5 February 2023

Available online 9 February 2023

0043-1648/© 2023 The Authors. Published by Elsevier B.V. This is an open access article under the CC BY license (<http://creativecommons.org/licenses/by/4.0/>).

in circular sawing has been investigated by Ersoy et al. [8] in 2005. They found that the metallic bond material shows predominantly abrasive wear behaviour. Two-body and three-body abrasion as well as the influence of varying stone types on the wear mechanisms was discussed in 2013 by Petrica et al. [9]. They correlated the specific wear energy of different rock types directly to their abrasive wear behaviour. In this study, it was concluded that the content of hard minerals within a rock composition is the dominant factor in the expected abrasivity in case of three-body abrasion, and the brittleness of the rock is the main factor in two-body abrasion. In 2018, Mostofi et al. [10] studied the wear characteristics of ID segments by performing core drilling experiments. They described polishing, fracturing, and sharpening as the three main diamond wear phases during core drilling through a granite rock. Additionally, they identified three-body abrasive wear of the bond material as root cause for the pull-out scenarios. All aforementioned studies investigated the effects of different stone and rock materials on the two-body and three-body abrasion. A recent publication from Fabbro et al. [11] investigated the wear behaviour of two different metallic alloys used as bond materials for diamond segments in a modified ASTM B611 wear test and comparing the results to diamond core drilling applications. They concluded that both segment types used, one ferritic-pearlitic and one copper based, showed a clear different wear behaviour tested against different counter bodies. Additionally, they observed a work hardened zone present at the copper based segment which acts as protective layer minimizing adhesive and abrasive wear at increasing forces and sliding speeds. Regardless of the success of ID segments, there is still a lack of understanding of the complex tribochemical and tribomechanical interaction at the metallic bond/concrete and metallic bond/rock interface. Diamond segments can be either exposed to solutions with acidic pH values in mining environments or to highly alkaline environments in the case of concrete drilling. In 2018, Dhir [12] characterized the waste water from mining sites as being acidic ranging between pH2 – pH4. However, publications investigating diamond segment wear while operating in alkaline media, like concrete water slurry, or acidic media, like in wet mining environment, have not been found. In 1974, Slyn'ko et al. [13] discussed the hydroabrasive wear of metals in an alkaline medium. They concluded that the intensity of hydroabrasive wear depends not only on the mechanical properties of the metals but also on their interaction with the medium and the presence of corrosion products. It was shown that corrosion processes on the surface are intensified by plastic deformation. Additionally, some metal alloys form thin passive films consisting of metal oxides/hydroxides. The destructive effect of abrasive particles is reduced by such films [13]. In 1985, Rengstorff et al. [14] published a study on friction and wear of metals in an alkaline medium. They observed that with increasing concentration of sodium hydroxide the friction and wear decreases accompanied by a decrease of iron oxide formation ( $\text{Fe}_2\text{O}_3$ ). One year before in 1984, Rengstorff et al. [15] presented a study on the friction and wear behaviour of iron at different concentrations of sulphuric acid. They concluded that over the entire acid concentration range, the highest direct corrosion loss was associated with the lowest coefficients of friction and showed that changes in wear can be significantly linked to corrosive effects in the acidic media. In diluted acid solutions (from 0.001 to 0.1 M) iron dissolution is rather low and metal losses are attributed to wear alone.

In this study, the ASTM B611-13 test is modified to achieve more realistic wear rates as well as wear patterns by varying the tribochemical and tribomechanical system. The influence of the microstructure on the wear behaviour at varying testing conditions is investigated and discussed. Subsequently, the laboratory test results are compared to core drilling experiments under real application conditions performed by Fabbro et al. [11].

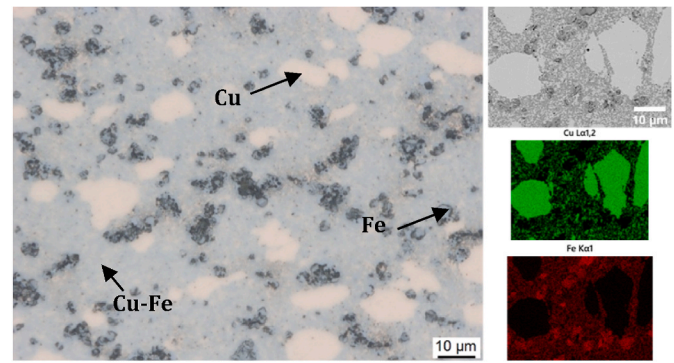


Fig. 1. Cross-section image of Segment A, etched with 2% Nital. Corresponding SEM image and EDS element mapping of Cu and Fe [11].

## 2. Specimen and Experimental Set Up

### 2.1. Test specimen

The metallurgical composition and the manufacturing process is identical to the test specimens investigated by Fabbro et al. [11], to ensure the comparability of these two studies. Segment A is a copper rich material solidified in a copper-iron binary system, shown in Fig. 1. Fig. 2 pictures a ferritic-pearlitic microstructure with sulphides hereafter referred to as Segment B.

### 2.2. Modified B611 - 13 test

The standard ASTM B611-13 (2018) [16] shown in Fig. 3, is a well-known test for investigating high-stress abrasion resistance. In this test, the specimen is pressed with a predefined force tangentially against a counter body, represented by a steel wheel rotating at a constant rpm. The wheel is equipped with flat or curved stirring paddles. These paddles ensure a sufficient slurry transport to the contact zone between counter body and specimen and prevent particle sedimentation.

For comparison between materials tested at different parameters, it is necessary to calculate the wear coefficient  $k$  in  $\text{mm}^3/(\text{Nm})$  discussed by Hutchings and Shipway [17]:

$$k = \frac{\Delta V}{L \cdot F} \quad (1)$$

where  $L$  represents the sliding distance in m,  $F$  the contact force in N and  $\Delta V$  the volumetric loss in  $\text{mm}^3$ .

All described modifications by Fabbro et al. [11], like the increase of slurry volume (from 1.0 l to 1.5 l) and abrasive particle concentration (7.5 g/ml) or to use a SSIC wheel to ensure a pure abrasive test environment, are done to simulate real application conditions. Additionally,

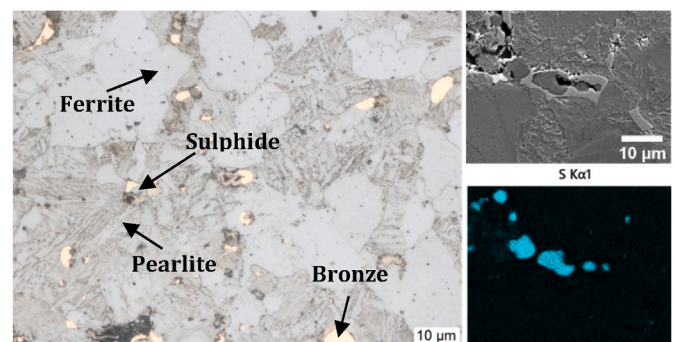


Fig. 2. Cross-section image of Segment B, etched with 2% Nital. EDX mapping detecting sulphides at grain boundaries [11].

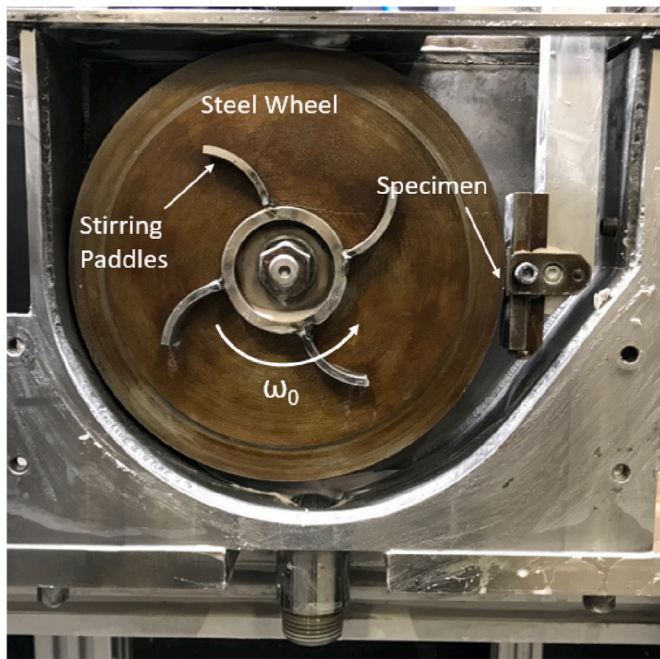


Fig. 3. The ASTM B611 test set up.

Table 1

Testing conditions for the modified B611-13 test.

Parameters: 200 N and 4 m/s					
Steel Wheel			SSiC Wheel		
pH13	pH7	pH2	pH13	pH7	pH2
Segment A			Segment A		
Segment B			Segment B		

no run-in period is performed to avoid damage of the specimen holder due to the high wear rate of the material. Table 1 provides an overview of the test parameters. The force of 200 N and 4 m/s sliding speed are representative for application related conditions.

### 2.3. Abrasive particles and slurry composition

The tribomechanical system is described by the counter body material, the applied force, sliding velocity, the abrasive particle concentration, the abrasive particle shape, and their hardness. For that reason, a synthetic slurry containing Silverbond M10 ( $d_{10} = 3,6 \mu\text{m}$ ,  $d_{50} = 21,7 \mu\text{m}$ ,  $d_{90} = 60,6 \mu\text{m}$ ) is used in this study. The abrasive consists of 99.6%  $\text{SiO}_2$  (Euroquartz Germany).

### 2.4. Tribochemical system

To adjust the pH value of the slurry to pH13 and pH2, two solutions of deionized water with small additions of sodium hydroxide (NaOH) and sulphuric acid ( $\text{H}_2\text{SO}_4$ ) are used. Therefore, the abrasive slurry mixture is prepared outside of the B611-13 rig and stirred with a magnetic mixer. 5 M NaOH or concentrated  $\text{H}_2\text{SO}_4$  are then added drop by drop until the desired pH value is reached. The pH values are measured with a Mettler Toledo SevenGo Duo pH meter. For pH7, solutions were used as obtained by mixing water and quartz particles.

### 2.5. Block on Ring test

The Coefficient of Friction (COF) measurements in Block on Ring configuration are performed using a modified UMT TriboLab mechani-

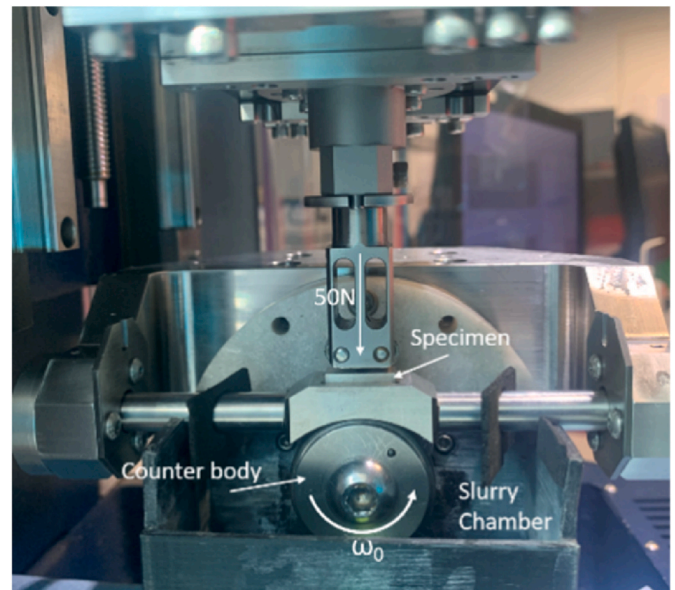


Fig. 4. The COF test set up.

cal tester (Bruker, Billerica, Massachusetts). The test setup with a sealed specimen chamber allows to measure the frictional forces and wear in variable pH environments. In contrast to the mild steel used in the B611 test, a quenched and tempered 100Cr6 counter body ( $\varnothing 35 \text{ mm}$ ) was utilized in this test. After a run-in period of 20 s with an applied force of 20 N, the normal force is set to 50 N. The test is then run for 120 s with an angular speed of 228 radians per second. The COF ( $\mu$ ) is calculated as explained by Bird and Chivers [18]:

$$\mu = \frac{F_R}{F_N} \quad (2)$$

Both, Segment A and Segment B samples are tested in slurries with different pH values. The test setup with an opened slurry chamber is shown in Fig. 4. The slurry chamber is filled completely with the solution to ensure a sufficient wetting of the segment-counter body interface. The contact mechanism can be described as Hertzian with a pressure of 90.5 MPa at the beginning, changing in conformal contact characteristic towards the end of the test.

### 2.6. X-ray photoelectron spectroscopy (XPS)

XPS high-resolution detail scans of the tested samples with focus on iron, sulphur, carbon, oxygen and sodium are acquired on two positions (centre and border) in the worn area. Additionally one untested sample hereafter referred to as "reference" has been investigated.

The used device is a Phi5000 VersaProbe spectrometer (ULVAC-PHI, INC.) equipped with a  $180^\circ$  spherical capacitor energy analyzer and a multi-channel detection system with 16 channels. The spectra are acquired at a base pressure of 5–10 $\cdot$ 10 $^{-8}$  Pa using a focused scanning monochromatic Al-K $\alpha$  source (1486.6 eV) with a spot size of 200  $\mu\text{m}$  and 50 W. The data is analyzed using the program CasaXPS [Version 2.3.16 [www.casaxps.com](http://www.casaxps.com)] and the signals are integrated following the Shirley background subtraction.

As a result, the measured amounts are given as apparent normalized atomic concentrations and the accuracy under the chosen condition is approximately  $\pm 10\%$ .

### 3. Results and discussion

#### 3.1. Wear coefficients

The wear coefficients obtained with the modified B611-13 test at different pH values of the slurry are shown in Figs. 5 and 6. A clear change in the wear behaviour when comparing the two segment materials can be observed. For both segment types the wear coefficients decrease when changing the pH of the surrounding media from pH7 to pH13 or pH2 using the steel wheel. The wear coefficient for the copper-rich Segment A at pH2 is  $0.05 \text{ mm}^3/(\text{Nm})$ , half of the wear coefficient observed at pH7 with  $0.1 \text{ mm}^3/(\text{Nm})$ . A similar trend but more pronounced can be seen in case of the iron-rich Segment B. Here, the wear coefficient is  $0.10 \text{ mm}^3/(\text{Nm})$  at pH2 and  $0.22 \text{ mm}^3/(\text{Nm})$  at pH13 compared to the value obtained at pH7 with  $0.49 \text{ mm}^3/(\text{Nm})$ .

For the SSiC the values are  $0.01 \text{ mm}^3/(\text{Nm})$  in all pH regimes of Segment A and  $0.03 \text{ mm}^3/(\text{Nm})$  at pH7 and pH13 down to  $0.01$  at pH2 of

Segment B. The reason for the low wear coefficients using the SSiC wheel, is described in detail in previous studies by Fabbro et al. [11] and can be explained by different mechanical and chemical properties of the S355 steel compared to the SSiC. The diamond like tetrahedral crystal structure of SiC is resulting in a low chemical affinity to the metallic segment material. Additionally, SSiC is resistant against different kinds of acids and alkaline solutions as a result of the presence of a protective  $\text{SiO}_2$  film, as concluded by Cook et al. [19].

A comparison of the wear coefficients obtained in core drilling experiments [11] to the above described coefficients is listed in Table 2. By changing the tribochemical system to pH13, similar wear coefficients are determined as in the real drilling experiment. For instance, Segment B shows with  $0.22 \text{ mm}^3/(\text{Nm})$  drilled in reinforced concrete the same wear coefficient as tested at pH13. Segment A shows a slightly higher value of  $0.07 \text{ mm}^3/(\text{Nm})$  tested at pH13 compared the corresponding reinforced concrete core drilling with  $0.05 \text{ mm}^3/(\text{Nm})$ . Segment A and Segment B reveal a clear decrease of the wear coefficients in the pH13

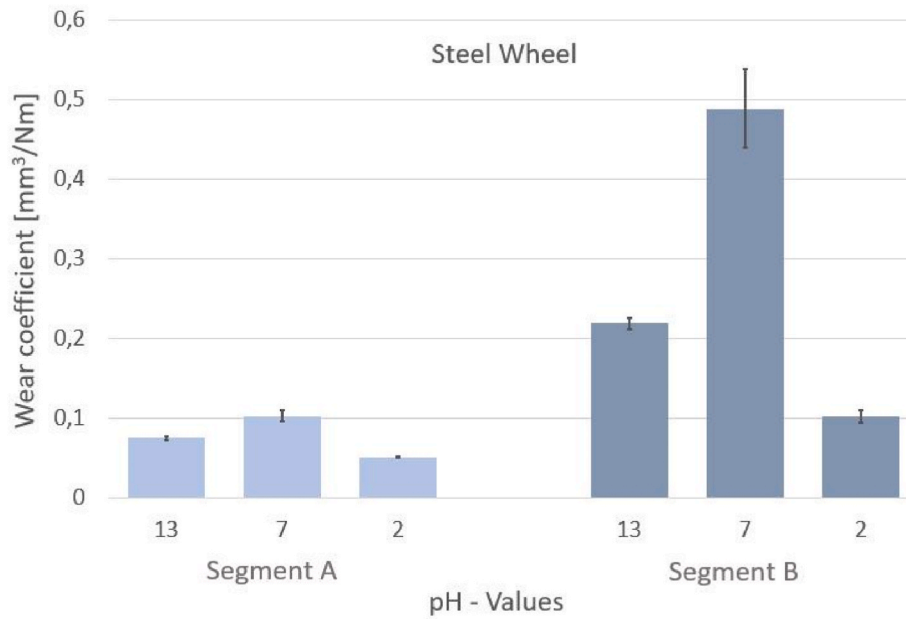


Fig. 5. Wear coefficients obtained at different pH values tested against the steel wheel.

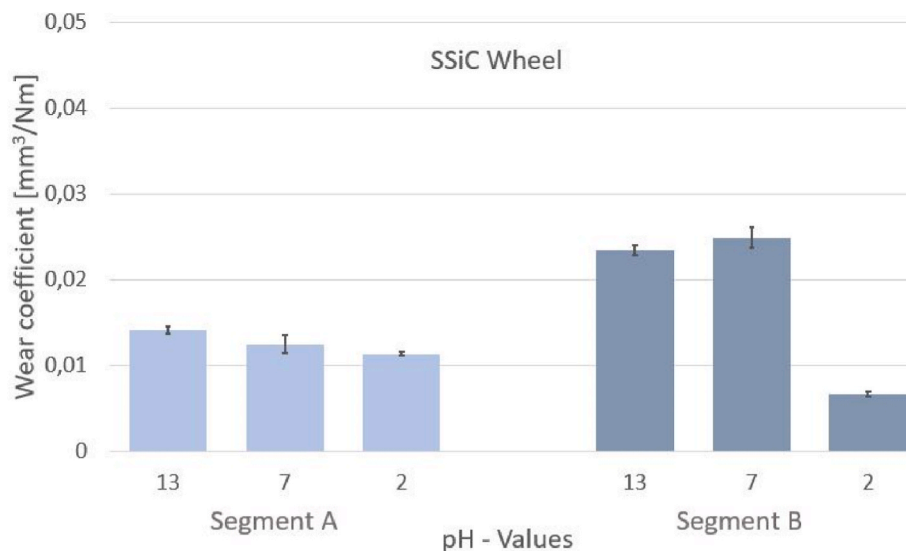


Fig. 6. Wear coefficients obtained at different pH values tested against the SSiC wheel.

**Table 2**  
Overview of the wear coefficients obtained in real core drilling experiments [11] and in pH B611-13 laboratory test against the steel wheel.

	Core drilling (pH13) [mm <sup>3</sup> /(Nm)]	pH13 [mm <sup>3</sup> / (Nm)]	pH7 [mm <sup>3</sup> / (Nm)]	pH2 [mm <sup>3</sup> / (Nm)]
A	0.05	0.07	0.10	0.05
B	0.22	0.22	0.49	0.10

laboratory test and a satisfying agreement with the values determined in concrete core drilling applications at pH13.

3.2. Microscopic investigation of wear tracks

Fig. 7 displays stereomicroscopic overview images of the wear tracks on both segment materials tested against both wheel types at different pH values. On Segment A, adhesive and abrasive wear can be observed when tested against the steel wheel. The tendency for adhesive wear

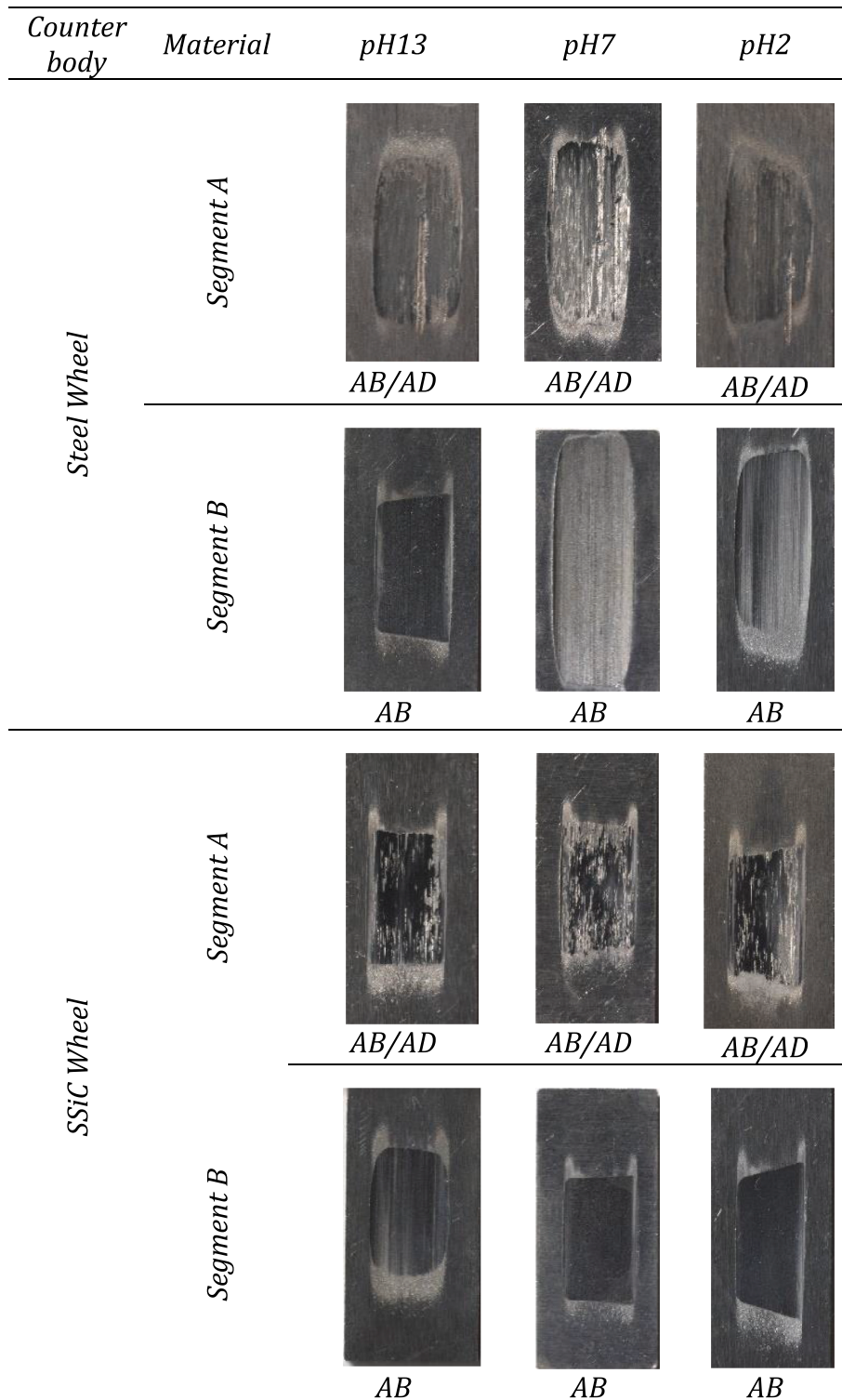


Fig. 7. Stereomicroscopic images of the worn surfaces (AD = adhesive wear; AB = abrasive wear). Each sample is 10 mm wide.

indicated by seizure marks is reduced when changing the pH value from pH7 to pH2 or pH13.

The iron-based Segment B is less prone to form adhesive wear under these test conditions compared to copper-rich Segment A. Three-body abrasion can be observed at pH7 and pH2 tested against the steel wheel. The other wear scars are mainly characterized through abrasive wear. Microscopic SEM images of the wear tracks are shown in Fig. 9. The copper containing Segment A shows adhesive wear with snout formation in combination with abrasive wear characterized by micro-ploughing. The aforementioned wear patterns are observed for tests against the steel wheel at pH7 and pH2. The tendency to snout formation decreases with increasing the pH value to pH13 showing a higher percentage of micro-ploughing, illustrated in Fig. 9a–c. Images of Segment B tested against the steel wheel are shown in Fig. 9d–f. Plastic surface deformations in combination with micro-cutting and particle indentations due to three-body abrasion can be observed at pH2 and pH13 as shown in Fig. 9e and f. A slightly different wear pattern is depicted in Fig. 9d. By changing the pH value to pH13, the iron-rich Segment B is additionally characterized by snout formations and embedded SiO<sub>2</sub> particles from the slurry.

In this configuration the influence of the pH value is less pronounced compared to the steel wheel. Segment A tested against the SSiC is illustrated in Fig. 9g–i and reveals predominantly abrasive wear characterized through micro-cutting. On the contrary, the wear pattern of Segment B tested against the SSiC wheel, is characterized by snout formations at all pH values, in combination with micro-cutting. Embedded SiO<sub>2</sub> particles can be found at all worn surfaces of both segment types tested against the SSiC wheel although the amount of SiO<sub>2</sub> particles is less at pH13.

In general, the wear rates increase significantly using the steel wheel. This is a result of the different mechanical properties of the SSiC wheel compared to the steel wheel. The hardness of the segment material is with 2–4 GPa comparable high compared to the hardness of the steel wheel with 1.5–1.8 GPa [20]. This results in an increase of adhesive wear by testing against the steel wheel. In contrary, the hardness of the SSiC wheel is with 23 GPa [21] significant higher compared to the hardness of the tested samples. This and the low chemical affinity to metal alloys of SiC due to its diamond like tetrahedral structure, results in predominantly abrasive wear [11].

### 3.3. Coefficient of friction (COF)

The coefficients of friction for both segment types measured at pH2, pH7 and pH13 are shown in Fig. 8. The results reveal a dependency of the friction coefficient on the pH value. The COF for copper-rich Segment A ranges between 0.26 for pH2 and 0.55 for pH7. Iron-rich Segment B shows COF ranging from 0.16 at pH2 to 0.31 at pH7. Both segment types indicate a similar trend with the highest value at pH7, the second highest at pH13 and the lowest COF at pH2.

In case of high pH, the findings can be explained by the formation of low friction oxide/hydroxide film in NaOH. In case of the acidic test regime, the H<sub>2</sub>SO<sub>4</sub> acid results in iron sulphate film formation at the wheel and segment interface, illustrated in Fig. 10. The influence of inorganic metallic sulphates on the friction, wear and seizure characteristics was investigated by Jain and Shukla [22]. They pointed out, that metallic sulphates result in a low friction film with anti-seizure properties.

### 3.4. X-ray photoelectron spectroscopy (XPS)

The atomic concentrations of the selected elements measured on the worn surface of the tested samples are listed in Table 3. The main detected elements for the reference sample are C, O and N which is an indication for a >5 nm thin organic layer on the surface. Measured C-compounds mainly origin from organic contamination of the samples. All tested samples show lower carbon concentration on the surface compared to the reference sample.

Sulphur in the form of a sulphate component can be found on the sample tested at pH2. Sodium is detected in the worn area only for samples tested at pH13, indicating hydroxide formation in the NaOH solution. The iron concentration is in the same range for the samples tested at pH13 compared to pH2 and pH7 by showing the lowest carbon concentration for all analyzed samples. However, iron detected from the substrate is mainly detected as a thin oxide layer.

Fig. 11 shows selected XPS-spectra for all tested samples at different positions. It is possible to identify the Na 1s for pH13 and the S 2p for pH2 signal.

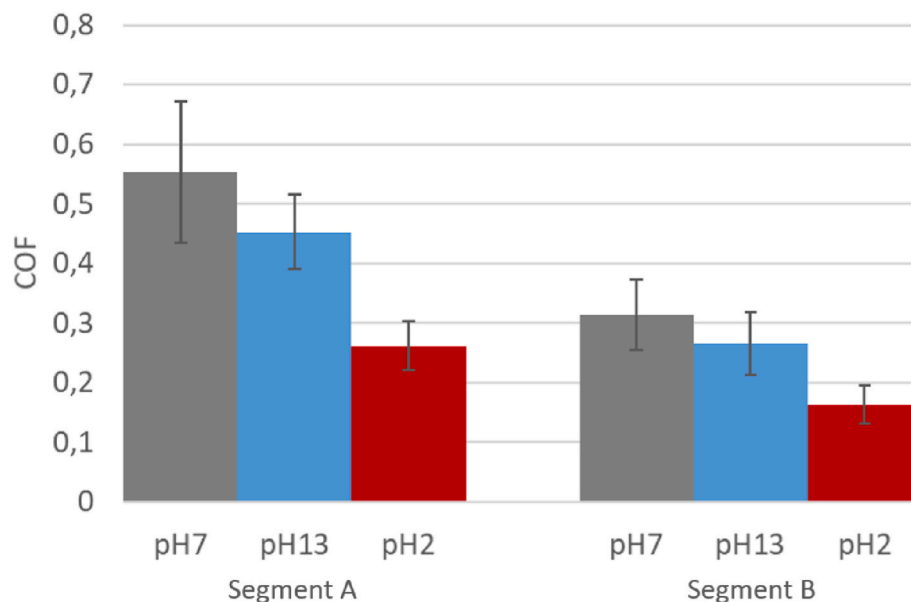


Fig. 8. COF of both segment materials at different pH values with the corresponding standard deviation tested in an abrasive slurry environment.

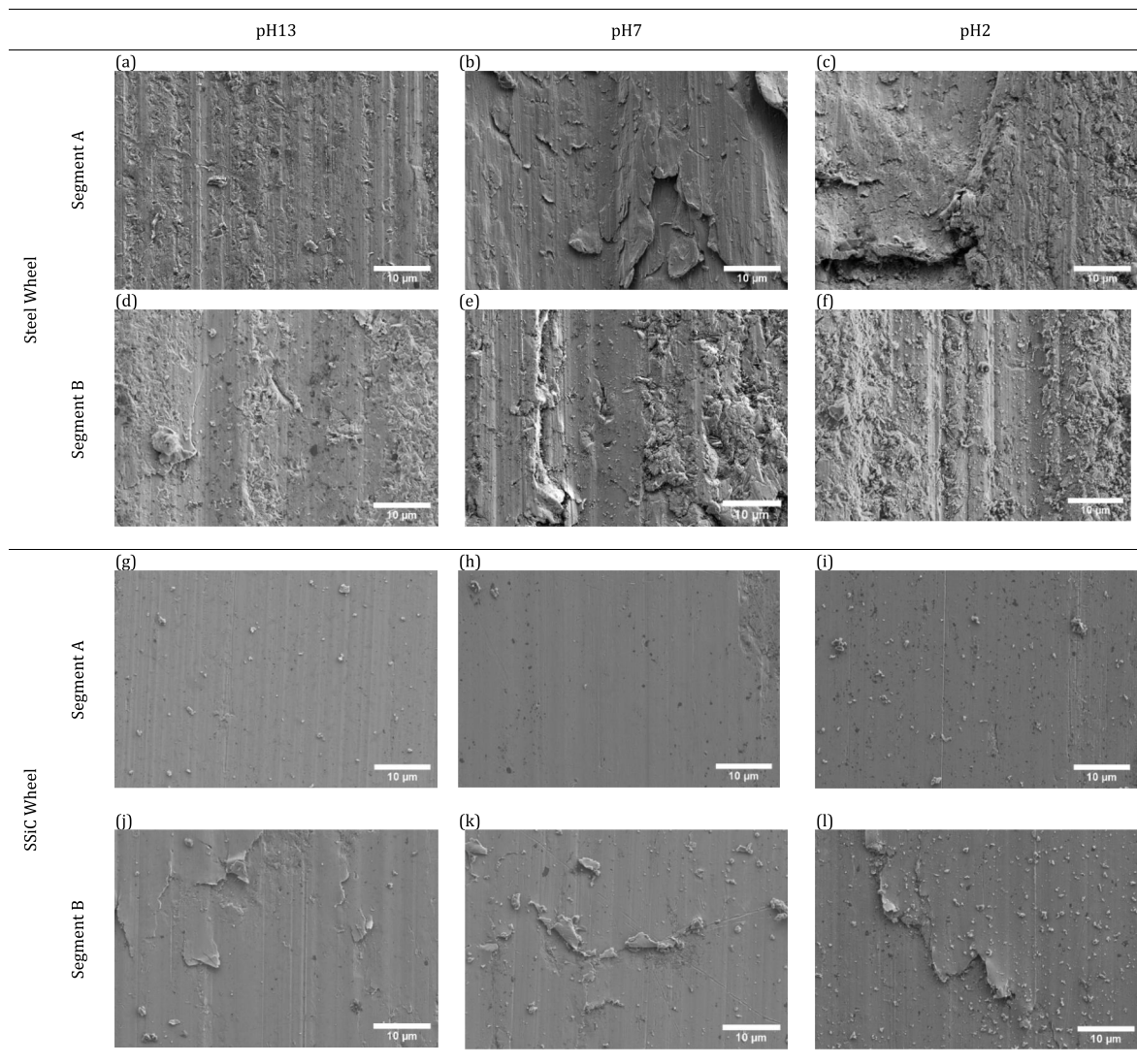


Fig. 9. SEM images of wear tracks of Segment A and Segment B tested with different pH values and counter bodies. (a)–(c): Segment A with (a) pH13, (b) pH7 and (c) pH2 and Segment B with (d) pH13, (e) pH7 and (f) pH2 against steel wheel. (g)–(i): Segment A with (g) pH13, (h) pH7 and (i) pH2 and Segment B with (j) pH13, (k) pH7 and (l) pH2 against the SSiC.

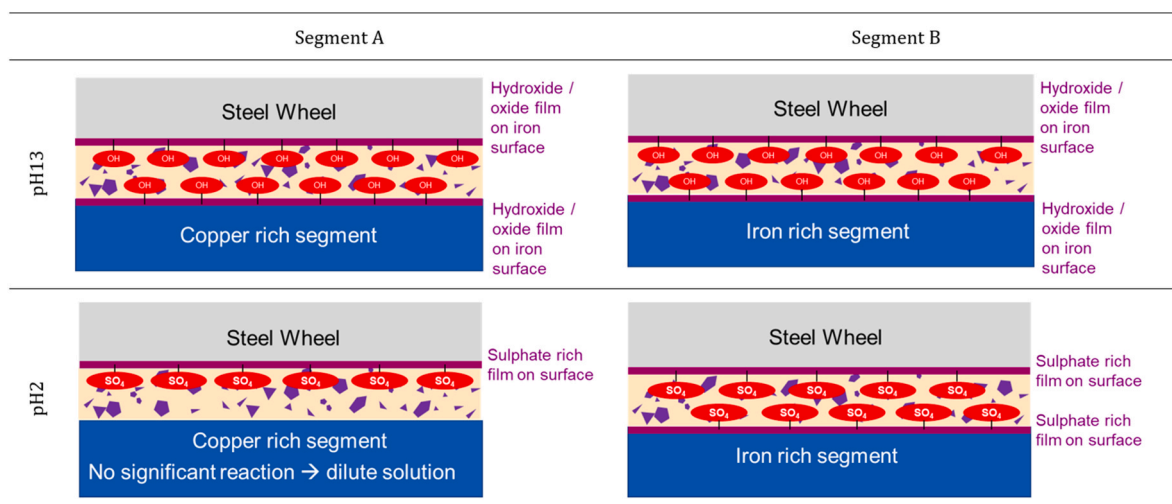
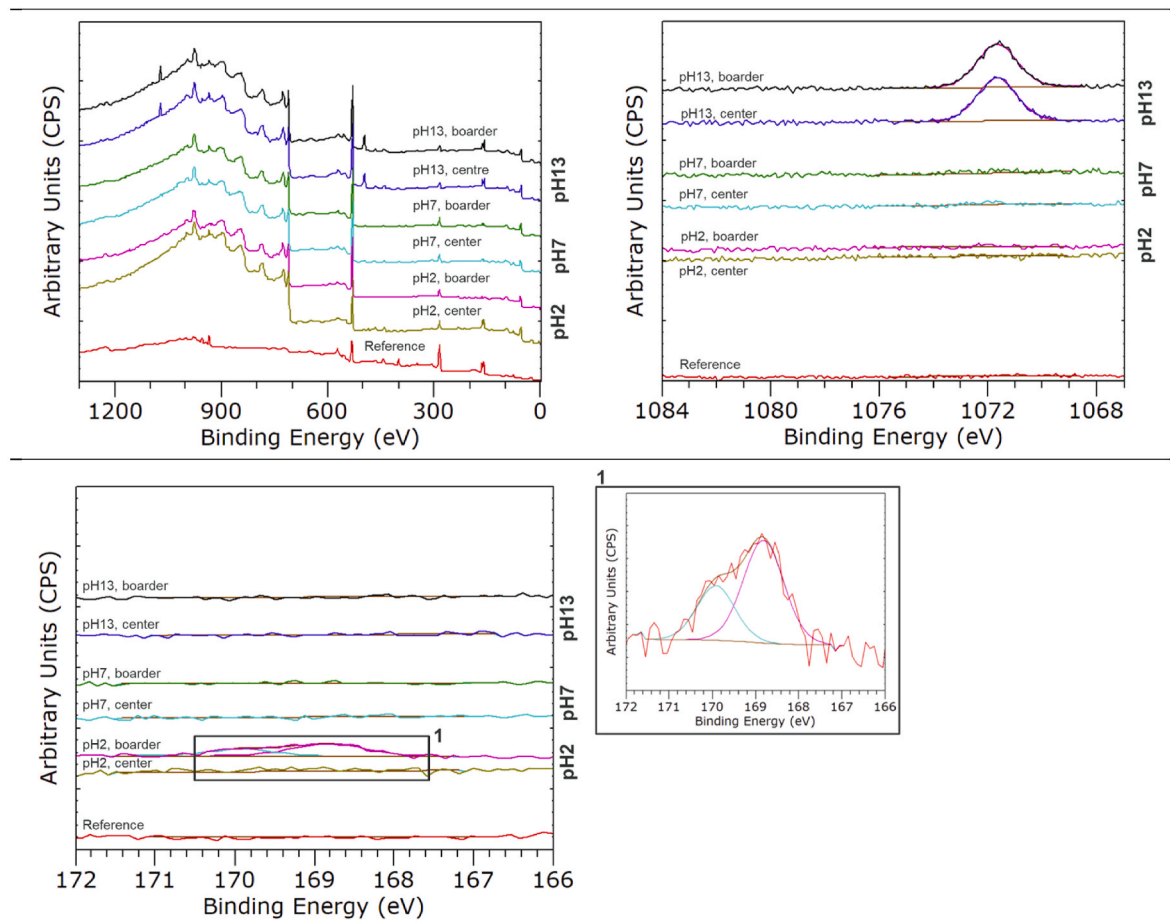


Fig. 10. Illustration of the low friction film formation at pH13 and pH2 in the steel wheel test.



**Table 3**  
Normalized atomic concentration (at.%) of selected elements detected on the surface of the 7 measuring positions.

At.-%	Fe	S	C	O	Na
Reference	1.7	0	62.9	19.4	0
pH2, centre	23.4	0	27.6	46.1	0
pH2, boarder	19.5	1.7	22.5	54.6	0
pH7, centre	18.5	0	24.5	54	0
pH7, boarder	18.6	0	25	53.2	0
pH13, centre	22	0	16.2	51.3	6.8
pH13, boarder	21.2	0	18.7	50.2	6.7



**Fig. 11.** XPS spectra for the samples tested at different pH values, measured at the centre and border position. a) overview of all spectra for full binding energy range; b) spectra for Na 1s; c) spectra for S 2p with detail view for pH2.

#### 4. Conclusion

A novel abrasive test approach for metallic matrix alloys using a B611-13 test with slurries at various pH has been developed. Two segment materials, one copper based (Segment A) and one ferritic-pearlitic segment (Segment B) have been investigated. In addition to the wear investigations at different tribochemical conditions, COF measurements were conducted in slurries with abrasive particles. Furthermore, microscopic investigations and XPS measurements of the worn surfaces were carried out. It was possible to show, that the determined wear coefficients at pH13 agree well with experimental data from real coring applications. In summary, the main conclusions drawn from this research are described as follows:

- The two different segment materials showed a change in wear behaviour by changing the pH regime from pH7 to pH13 or pH2. In

case of pH13, wear reduction is caused by the formation of a low friction film consisting of iron hydroxide/oxide, which is known to reduce friction and is quickly formed again once destroyed by the abrasives. A lower wear coefficient compared to the neutral media was also observed at pH2. The attack by the dilute acid at pH2 is negligible regarding pure metal loss, but still sufficient to cause changes in the boundary layer that have a friction-reducing effect additionally caused by the formation of inorganic iron sulphates. The metallic sulphate formation is more pronounced on the iron-rich segment. It can be assumed that this effect is present on both surfaces, steel wheel and segment, contributing to a lower friction and wear coefficient. In contrary to the copper rich segment, the pH value is not acidic enough to significantly react with the copper surface to create a sulphate film. Therefore, the low-friction film is created on the steel wheel surface only.

- Comparing the light microscopic images of Segment A and Segment B tested at different pH values, the copper based segment shows abrasive and adhesive wear marks, especially at pH7. The tendency to adhesive wear is reduced when changing to pH2 or pH13 as a result of the anti-seizure properties of the sulphate and the low friction properties of the oxide/hydroxide film. In contrary, iron-rich Segment B is mainly characterized by three-body abrasion and there is no clear indication for adhesive wear. The influence of different pH values on the wear mechanism is less significant when the SSiC wheel was used. This can be explained by the fact, that the pH value influences the tendency to adhesive wear, which was mainly observed by testing with the steel wheel.
- The results determined by the COF experiments show a clear dependency of both segment types on the pH value. The highest COF value is observed when testing at pH7 followed by pH13 and pH2. This is in accordance with the wear coefficients and the observed wear patterns.
- The XPS results obtained by measuring the samples tested at different pH values in the COF experiments confirm the observations from the microscopical investigation and mechanical tests. It is possible to measure sulphur in from of a sulphate compound only on the pH2 samples. Whereas, a thin iron oxide film and sodium hydroxides could be detected on the sample tested at pH13.

A potential subsequent work could be to change the pH value to the more extremes like pH1 and pH14. This in combination with another acid like hydrochloric acid instead of sulphuric acid, could deepen the understanding of different wear characteristics changing the tribochemical system.

#### Declaration of competing interest

The authors declare that they have no known competing financial interests or personal relationships that could have appeared to influence the work reported in this paper.

#### Data availability

No data was used for the research described in the article.

#### Acknowledgements

The authors gratefully acknowledge the Swiss government by supporting this work with the Innosuisse Research Project (No.27558.1) and Hilti AG by providing the ASTM B611-13 test equipment, diamond segment specimens and the synthetic slurry.

#### References

- [1] L.F.P. Franca, M. Mostofi, T. Richard, Interface laws for impregnated diamond tools for a given state of wear, *Int. J. Rock Mech. Min. Sci.* 73 (2015) 184–193, <https://doi.org/10.1016/j.ijrmms.2014.09.010>.
- [2] S.G. Moseley, K.P. Bohn, M. Goedicke, Core drilling in reinforced concrete using polycrystalline diamond (PCD) cutters: wear and fracture mechanisms, *Int. J. Refract. Met. Hard Mater.* 27 (2009) 394–402, <https://doi.org/10.1016/j.ijrmhm.2008.11.014>.
- [3] D. Miller, Rock Drilling with Impregnated Diamond Microbits:1-277, Ph.D. thesis, University of Cape Town, 1986, <http://open.uct.ac.za/handle/11427/4962>.
- [4] H.K. Tönshoff, B. Denkena, H.H. Apmann, J. Asche, Diamond tools in stone and civil engineering industry - cutting principles, wear and applications, *Key Eng. Mater.* 250 (2003) 103–109, <http://doi.org/10.4028/www.scientific.net/ke.m.250.103>.
- [5] D. Miller, A. Ball, The wear of diamonds in impregnated diamond bit drilling, *Wear* 141 (1991) 311–320, [https://doi.org/10.1016/0043-1648\(91\)90276-Z](https://doi.org/10.1016/0043-1648(91)90276-Z).
- [6] T. Xuefeng, T. Shifeng, The wear mechanisms of impregnated diamond bits, *Wear* 177 (1994) 81–91, [https://doi.org/10.1016/0043-1648\(94\)90120-1](https://doi.org/10.1016/0043-1648(94)90120-1).
- [7] M. Borri-Brunetto, A. Carpinteri, S. Invernizzi, Characterization and mechanical modeling of the abrasion properties of sintered tools with embedded hard particles, *Wear* 254 (2003) 635–644, [https://doi.org/10.1016/S0043-1648\(03\)00254-0](https://doi.org/10.1016/S0043-1648(03)00254-0).
- [8] A. Ersoy, S. Buyuksagic, U. Atici, Wear characteristics of circular diamond saws in the cutting of different hard abrasive rocks, *Wear* 258 (2005) 1422–1436, <https://doi.org/10.1016/j.wear.2004.09.060>.
- [9] M. Petrica, E. Badisch, T. Peinsitt, Abrasive wear mechanisms and their relation to rock properties, *Wear* 308 (2013) 86–94, <https://doi.org/10.1016/j.wear.2013.10.005>.
- [10] M. Mostofi, T. Richard, L. Franca, S. Yalamanchi, Wear response of impregnated diamond bits, *Wear* 410–411 (2018) 34–42, <https://doi.org/10.1016/j.wear.2018.04.010>.
- [11] S. Fabbro, L.M. Araujo, J. Engel, J. Kondratiuk, M. Kuffa, K. Wegener, Abrasive and adhesive wear behaviour of metallic bonds in a synthetic slurry test for wear prediction in reinforced concrete, *Wear* (2021), 203690, <https://doi.org/10.1016/j.wear.2021.203690>.
- [12] B. Dhir, Chapter 4 - biotechnological tools for remediation of acid mine drainage (removal of metals from wastewater and leachate), in: M.N.V. Prasad, P.J. de Campos Favas, S.K. Maiti (Eds.), *Bio-Geotechnologies Mine Site Rehabil*, Elsevier, 2018, pp. 67–82, <https://doi.org/10.1016/B978-0-12-812986-9.00004-X>.
- [13] A.I. Slyn'ko, G.A. Preis, N.A. Sologub, Hydroabrasive wear of metals in alkaline media, *Sov. Mater. Sci. a Transl. Fiz. Mekhanika Mater./Acad. Sci. Ukr. SSR.* 8 (1974) 133–136, <https://doi.org/10.1007/BF00731994>.
- [14] G.W.P. Rengstorff, K. Miyoshi, D.H. Buckley, Friction and wear of iron in corrosive media, *NASA Tech. Pap.* 1985 (1982) 1–17.
- [15] G.W.P. Rengstorff, *Sulfuric Acid Friction and Wear Sulfuric Acid*, 2018.
- [16] ASTM International, Standard Test Method for Determining the High Stress Abrasion Resistance of Hard Materials, vol. 13, 2018, pp. 1–6, <https://doi.org/10.1520/B0611-13R18>. Copyright.
- [17] I. Hutchings, P. Shipway, *Tribology: Friction and Wear of Engineering Materials*, second ed., Butterworth-Heinemann, 2017.
- [18] J.O. Bird, P.J. Chivers, 28 - friction, in: J.O. Bird, P.J. Chivers (Eds.), *Newnes Eng. Phys. Sci. Pocket B*, Newnes, 1993, pp. 235–237, <https://doi.org/10.1016/B978-0-7506-1683-6.50031-X>.
- [19] S.G. Cook, J.A. Little, J.E. King, Corrosion of silicon carbide ceramics using conventional and electrochemical methods, *Br. Corrosion J.* 29 (1994) 183–189, <https://doi.org/10.1179/000705994798267692>.
- [20] V. Läßle, *Einführung in die Festigkeitslehre*, 2016, <https://doi.org/10.1007/978-3-658-10611-9>.
- [21] P. Barick, A. Chatterjee, B. Majumdar, B.P. Saha, R. Mitra, Comparative evaluations and microstructure: mechanical property relations of sintered silicon carbide consolidated by various techniques, *Metall. Mater. Trans. A Phys. Metall. Mater. Sci.* 49 (2018) 1182–1201, <https://doi.org/10.1007/s11661-018-4486-6>.
- [22] V.K. Jain, D.S. Shukla, Study of the EP activity of water-soluble inorganic metallic salts for aqueous cutting fluids, *Wear* 193 (1996) 226–234, [https://doi.org/10.1016/0043-1648\(95\)06774-4](https://doi.org/10.1016/0043-1648(95)06774-4).